analytical chemistry

pubs.acs.org/ac Article

Fentanyl Assay Derived from Intermolecular Interaction-Enabled Small Molecule Recognition (iMSR) with Differential Impedance Analysis for Point-of-Care Testing

Zhe Wang,* Amit Nautiyal, Christopher Alexopoulos, Rania Aqrawi, Xiaozhou Huang, Ashraf Ali, Katherine E. Lawson, Kevin Riley, Andrew J. Adamczyk, Pei Dong, and Xinyu Zhang

Cite This: *Anal. Chem.* 2022, 94, 9242−9251 Read Online

ACCESS | Metrics & More | Article Recommendations | Supporting Information

ABSTRACT: Rapid and effective differentiation and quantification of a small molecule drug, such as fentanyl, in bodily fluids are major challenges for diagnosis and personal medication. However, the current toxicology methods used to measure drug concentration and metabolites require laboratory-based testing, which is not an efficient or cost-effective way to treat patients in a timely manner. Here, we show an assay for monitoring fentanyl levels by combining the intermolecular interaction-enabled small molecule recognition (iMSR) with differential impedance analysis of conjugated polymers. The differential interactions with the designed anchor interface were transduced through the perturbance of the electric status of the flexible conducting polymer. This assay showed excellent fentanyl selectivity against common interferences, as well as in variable body fluids through either testing strips or skin patches. Directly using the patient blood, the sensor provided 1%−5% of the average deviation compared to the "gold" standard method LC-MS results in the medically relevant fentanyl range of 20−90 nM. The superior sensing properties, in conjunction with mechanical flexibility and compatibility, enabled point-of-care detection and provided a promising avenue for applications beyond the scope of biomarker detection.

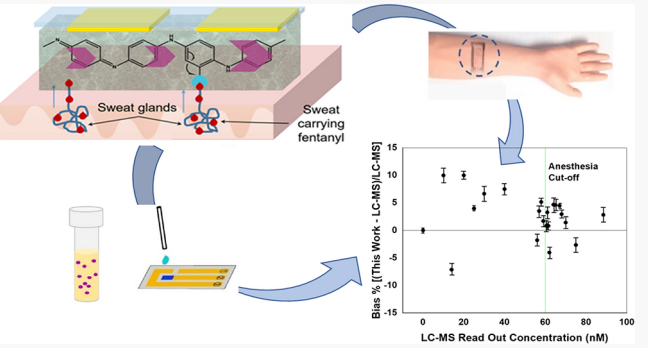

INTRODUCTION

Opioids represent one of many therapeutic options to treat chronic nonmalignant pain (CNMP) and have been among the most frequently prescribed medications in the United States since the 1990s, with hydrocodone being the second most dispensed medication overall as of 2015.[1] The fact that there are no medications available to address moderate to severe pains that are both equally efficacious and safer than opioids partially explains the explosion in opioid prescriptions for this population.[2,3] The use of chronic opioid therapy (C.O.T.) in patients with CNMP remains controversial because of insufficient trials (>12 months) demonstrating analgesic and functional benefits, in addition to mounting data that repeatedly highlight the (dose-dependent) hazards of C.O.T.: opioid misuse and abuse, opioid-related motor vehicle accidents, and unintentional deaths from overdosing.[4] However, in the current chronic therapy, drug tapering has emerged as a common intervention to mitigate the unfavorable long-term chronic therapy risk−benefit balance. It is a challenge to make timely and precise decisions based on the individuals, since the physician is mainly relying on the patient's report to conduct drug screening and dose titration (perhaps 30 days between appointments).[5,6] Furthermore, individuals' tolerances to overdose vary with age, state of health, how the substance was consumed, and a number of other factors.[7] Physicians who dispense controlled substances have a responsibility not to dispense to patients who may be at risk for abuse of these drugs; however, they have limited rapid and accurate detection tools to provide need-based doses for individuals.[8] The current toxicology methods used to measure drug concentration and metabolites require laboratory-based testing, which is not an efficient or cost-effective way to treat patients in a timely manner. There are no real-time tools, data, or models available for individual therapy. As a result, many overdoses originated from opioid prescriptions dispensed by doctors, soaring to 236 million prescriptions in 2016, which is three times the amount of opioids prescribed in 1999 and four times the amount prescribed by European counterparts in 2015.[9,10]

Received: January 3, 2022
Accepted: June 8, 2022
Published: June 23, 2022

https://doi.org/10.1021/acs.analchem.2c00017
Anal. Chem. 2022, 94, 9242−9251

As one of the common opioids, the fentanyl concentration recommended is located in a wide range where analgesia is about 12 nM in serum. For anesthesia, it is 60 nM, and abuse death has a mean concentration of only around 90 nM.[11−13] In order to accurately measure such small molecule concentrations, special separation processes have to be performed, combined with a detection method. The current confirmatory drug test involves either gas chromatography−mass spectrometry (GC-MS) or liquid chromatography−mass spectrometry (LC-MS),[14−16] which are time consuming and not suitable for point-of-care testing (POCT). Not only for proper assessment of the severity of overdose/double-dipping but also for appropriate therapeutic decision making, there is a pressing demand for noninvasive/low-invasive POC fentanyl monitoring techniques.[14] Recently, the techniques based on Raman vibrational spectroscopic have been designed for portable detection, as it provides a molecularly specific fingerprint that can be used for the identification and quantification of a compound.[17−19] However, the Raman effect for an analyte within a biofluid is generally weak, and spectroscopy-based screening has limitations when applied in POC situations because of high maintenance, instrument cost, and failure in high threshold tests.[20] Electrochemical (EC) biosensors provide fast measurement with high sensitivity, low cost, and a high degree of miniaturizability for POC testing and field decision making, even for the airborne trace compounds.[21−23] Due to limited specificity for complex samples, traditionally, in terms of small molecule clinical testing, EC devices have often been used as attachments to separation devices, such as GC, LC, and microfluidics, for postseparation detection.[24,25]

In natural processes, the recognition of small molecules through noncovalent interactions is well studied, such as nucleic acids are selectively paired through three to four intermolecular hydrogen bonds that grant high molecule recognition for the precise construction of DNA and RNA structures.[26,27] Inspired by this high specificity of 3-D molecular pairing, we have generated an environment where selective adsorption of small molecules is more competitive in comparison to other interfering molecules. This method provided greater than 98% accuracy of acetaminophen (AP) measurement on a blood testing strip.[24] The anchor molecule was designed to have multiple hydrogen bond patterns, with 1:1 stoichiometry corresponding to the targeted small molecule in three-dimensions, called multihydrogen bond-manipulated small-molecule recognition (eMuHSiR). However, due to fentanyl's weak redox activity and comparatively lower biological concentration, eMuHSiR would be unsuitable for the quantification of fentanyl.

As one of the most studied conducting polymers, polyaniline (PANI) is extremely sensitive toward chain conformations arising from π-orbitals structures.[26,27] Since the analyte's attachment can alter the delocalized electrons that further modify the electronic structure of PANI, the binding of an analyte can be converted to a PANI electrical signal providing rapidly measurable results.[28,29] Further, the flexibility of a polymer and adjustable PANI structure can be easily tuned for universal application with a given sensitivity of detection.[28,30]

In this work, semiconductive PANI was employed to improve sensitivity toward fentanyl detection. We designed and fabricated an anchor layer for fentanyl absorption based off the principle of eMuHSiR. L-Arginine-PANI acts as an anchor site to adsorb fentanyl onto the sensor interface. Instead of strictly hydrogen bonds, multiple noncovalent bond (H-bond, polar−π, cation−π, and π−π interaction) patterns were designed and utilized for fentanyl structural adsorption, named intermolecular interaction-enabled single molecule recognition (iMSR). This technique was verified to be independent of environmental pH, further described by density functional theory (DFT), and explored using spectroscopies. The adsorbed fentanyl was quantified through electrochemical impedance spectroscopy (EIS), a sensitive technique suitable for measuring the electronic changes of semiconductors, such as PANI polymer. This EC-based sensor was first trained in phosphate-buffered saline (PBS) solutions and then engineered to test in serum and artificial tears, in addition to an attachable sensor for in situ monitoring through artificial skin perspiration. Finally, the sensor was validated in clinical human blood samples.

EXPERIMENTAL SECTION

Computational Methodology. The interaction between arginine-bound PANI and fentanyl has been investigated with quantum chemical methods using density functional theory (DFT) with an empirical dispersion correction.[28,29] The adsorption complexes of various configurations of fentanyl (adsorbate) and arginine-substituted polyaniline hexamer (AS-PANI) (adsorbent), representing the sensor surface were investigated utilizing DFT calculations as implemented in the Gaussian 16 software. The generalized gradient approximation (GGA) with the Becke/Lee, Yang, and Parr (BLYP) exchange-correlation functional has been used with the 6-31G(d) basis set. The Grimme dispersion with the original D3 damping function was used to provide an improved description of the nonlocal nature of the electron correlation, particularly hydrogen bonds and van der Waals interactions.[30] Implicit solvation using a self-consistent reaction field (SCRF) with the Conductor-like Polarizable Continuum Model (CPCM) was employed with the dielectric constant of water (ε = 78).[31] (Supporting Information SI-1)

Materials. Aniline, L-arginine, and platinum (Pt) gauze (100 mesh, 99.9% metal basis) were purchased from Sigma-Aldrich, USA. Sulfuric acid (SA) was obtained from Fisher Scientific. A gold (Au) working electrode (2 mm diameter) was purchased from CH Instrument. Human serum was obtained from Sigma-Aldrich (from human male AB plasma, USA origin, sterile filtered). Artificial tears (GenTeal preservative-free teardrops) were purchased from Amazon. Artificial sweat was prepared following the procedure reported elsewhere.[32] Other chemicals were purchased from Sigma Aldrich. All chemicals were used as received. Fentanyl (Fent) solution (1 mg/1 mL of methanol) was purchased from Sigma-Aldrich. It was provided in a 1 mL ampule. Fentanyl was diluted to 100 μM in a 0.01 M phosphate buffer (Sigma-Aldrich) prior to use. The deidentified blood samples were collected by the School of Medicine, Louisiana State University, Biobank from the clinic.

Sensor Fabrication. The VersaSTAT 4 potentiostat galvanostat was used in this work. All the EIS measurements were conducted at open circuit potential. The frequency scan range is from 100 K Hz to 0.01 Hz with 0.01 V amplitude. Incubation time is 500 s, and the total sample volume is 5 mL. The electropolymerization of aniline was carried out in a single compartment electrochemical cell containing 0.1 M aniline and 0.5 M sulfuric acid. Potentiostatic deposition was carried out by applying 1 V for 10 mins to obtain PANI coating. It was further rinsed with DI water and dried at room temperature for

https://doi.org/10.1021/acs.analchem.2c00017
Anal. Chem. 2022, 94, 9242−9251

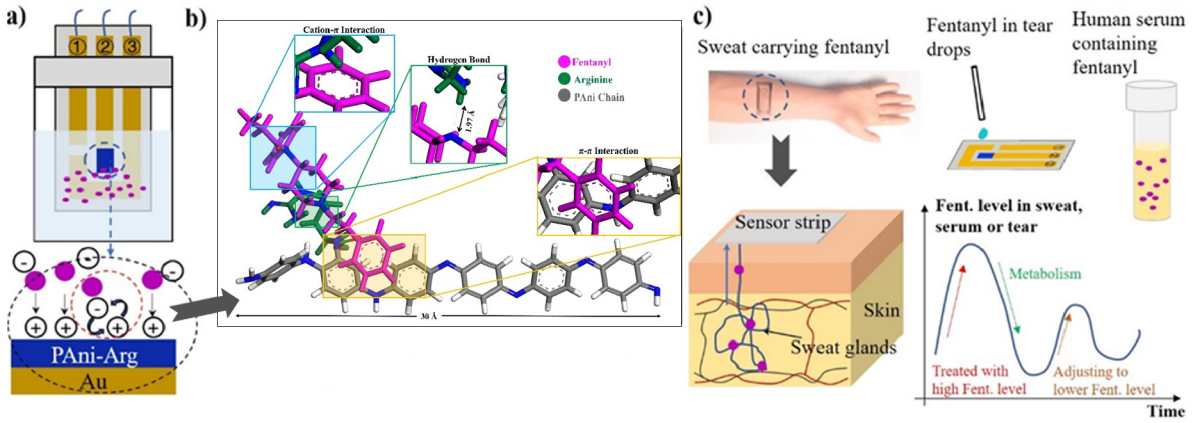

Figure 1. Interface design and fabrication for POCT setting. (a) Graphical representation of fentanyl interaction at sensor surface (purple dots are fentanyl molecules, and 1, 2, and 3 on sensor strip represents reference, working, and counter electrode, respectively). (b) Various noncovalent interactions between functional groups of fentanyl and arginine-bound PANI in example configuration 8. L-Arginine-facilitated binding between fentanyl and polyaniline leads to a surface charge difference on the sensor surface. (Fentanyl is represented by purple, functional arginine by green, PANI chain by gray, and cation−π interaction between fentanyl and arginine, hydrogen bond between arginine and fentanyl, π−π interaction between fentanyl, and PANI chain). (c) Schematic representation of application of our sensor in bodily fluids that can prevent overdosage (sensor material is touching the skin in contact with sweat; purple dots in human serum represents fentanyl).

2−4 h. This dried PANI film was then treated with aqueous ammonia to obtain dedoped PANI (Emeraldine Base). Further, arginine addition on PANI (AS-PANI) was carried out by applying 1 V for 10 min to a PANI (Emeraldine Base) film in a 0.9 M L-arginine solution. (Supporting Information SI-2) The resultant film was rinsed with DI water and dried at 50 °C for 10−12 h prior to use. All potentials were measured using Ag/AgCl as a reference electrode unless otherwise mentioned.

Interface and Sample Characterization. The interaction of arginine and fentanyl was confirmed using a Beckmen Coulter DU-800 UV−vis spectrophotometer and Thermo Nicolet 6700. LC-MS tests were performed with Agilent 6520 Q-TOF LC-MS.

Strip and Patch Fabrication. Polytetrafluoroethylene (PTFE) (0.81 mm thick) was purchased from Thermo Scientific and polydimethylsiloxane (PDMS) (1/25 in. thick) from Siliconlms. The Au electrode was deposited by a sputtering technique (HUMMER XP, Anatech LTD). To make a mask for the sputtering, the pattern of the mask was designed by a 3D modeling online resource. Autodesk Tinkercad, and the mask was then fabricated by a 3D printer, Ultimaker 3. After attaching the mask to the PDMS substrate, the substrate with the mask was moved in the sputtering equipment, and a layer of 300 nm target materials (Au/Pd ∼ 70/30) was deposited on the substrate (Figure 1a) for further blood and sweat testing (Figure 1b).

Sensor Testing. Concerning the batch-to-batch differences in our sensors, our method of quantification utilizes the change from the baseline as opposed to a universal baseline. This method allows batch-to-batch differences between sensors to be negated, as generated individual baselines for each sensor. The sensor was stored in PBS, and a baseline was be generated prior to use. The samples were subsequently added into the PBS solution, and a new impedance measurement was retrieved. This change in impedance was used in conjunction with the calibration curve to quantify the concentration of fentanyl.

RESULTS AND DISCUSSION

iMSR Anchor Structure Design and DFT Calculation. In previous research, we have demonstrated that an arginine anchor site design could be utilized to quantify acetaminophen concentration through electrochemical techniques, and fentanyl contains the *N*-phenylacetamide structure, which could initiate two hydrogen bondings with the L-alanine group of arginine as proved.[33] Another end of azanecarboximidamide in arginine is available for chemical crafting and connecting the other group pairing with the phenethylpiperidine structure of fentanyl to acquire the structure adsorption. The PANI structure was selected since the aniline ring of PANI provided π−π interactions with the benzene ring of fentanyl, and *N*-phenylacetamide from arginine could craft on the chain through the reported method (Supporting Information SI-1). Here, small molecular recognition was achieved through multiple intermolecular interactions. The DFT calculations were applied with an empirical dispersion correction and multiple interactions where noncolvenent bonds patterns between the nitrogen atom of the piperidine group of fentanyl and the guanidino group of AS, polar−π and cation−π interactions between the guanidino group of AS and the phenyl group of fentanyl, H-bond with the PANI backbone, and π−π interactions between the phenyl groups of fentanyl, and the PANI backbone were observed within the different configurations of the complex formed at the interface of the sensor.[34,35] As shown in Supporting Information SI-1, the Fent-AS-PANI complex is formed and stabilized by a noncovalent bond pattern in the interface (Figures 1a and b). To generate a robust analysis of the different binding interactions between the fentanyl molecule and AS, calculations have been carried out for nine different configurations of the complexes, and within each configuration, four zwitterionic states of functional arginine were studied to determine possible pH effects (Figures S1 and S2). The interaction energies between fentanyl and AS-PANI are found to vary from −0.38 to −2.38 eV, with a mean value of −1.19 eV (Tables S1 and S2). Our calculations are in line with the literature that agrees that the cation−π interactions between the positively charged guanidinium group of functional

https://doi.org/10.1021/acs.analchem.2c00017
Anal. Chem. 2022, 94, 9242−9251

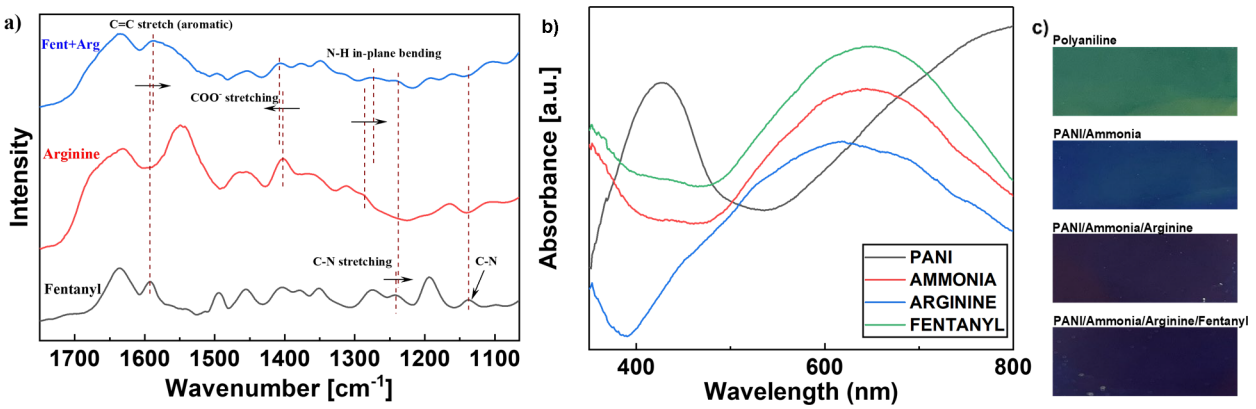

Figure 2. Molecule interaction characterizations with FTIR and UV. (a) FTIR spectrum of fentanyl, functional arginine, and functional arginine + fentanyl composite solution. (b) UV−vis and characterizing the sensing interface at various stages of its fabrication on ITO glass. (c) Color images of sensing layer fabrication on ITO glass.

arginine and the π-bonding of the phenyl rings of the fentanyl molecules also play key roles in these relatively strong interactions or binding energies of the complexes.[34] In Table S1, there are four very strong interactions (binding energy ranges from −2.378 to −1.959 eV) that are observed for the third zwitterionic state of configurations 1, 4, and 8 and for the first zwitterionic state of configuration 2. These strong interactions have arisen due to a spontaneous proton transfer from the guanidinium group of arginine to the piperidine group of fentanyl in addition to the other noncovalent interactions previously mentioned. Since the strength of the hydrogen bond between nitrogen and nitrogen/oxygen ranges from −0.0976 to −0.2953 eV[36] and the average binding energy in the fentanyl and AS-PANI complex was −1.19 eV, it indicates that the average intermolecular reaction between fentanyl and AS-PANI is approximately four hydrogen bonds, which are more than sufficient to form a stable paring as indicated. Additionally, the specific steric structure of the anchor structure design and PANI would prevent strong adsorption from the interference molecules, which would not cause the PANI electric structure to change.

It should be noted that our computational findings suggest excellent reproducibility in sensor performance (independent of pH variations). Although pH variations may modify the zwitterionic states of the functional group of arginine, it does not significantly influence the noncovalent binding energy (Tables S1, S2, and S3and Figure S3 and S4). These noncovalent interactions were strongly dependent on configurations of fentanyl and AS-PANI clusters (depicted in Figure S3). These findings showed the sensor built with this sensing mechanism could be used in physiological pH too, i.e., in different body fluids. Figure 1c shows the potential use of our sensor as a test strip and skin patch to detect/monitor fentanyl concentration in sweat, human tears, or human serum. This helps health workers to carefully adjust the dosage according to the metabolism of individuals.

Sensing Layer Fabrication and Characterization. Typically, PANI shows the transformation of its three different oxidation states (leucoemeraldine, emeraldine, pernigraniline) during cyclic voltammetry in the strongly acidic electrolyte (Supporting Information SI-2 and Figure S5a). This change in oxidation states can be seen in the voltammogram as redox peaks in positive or negative scans.[37] The fabrication of the sensing interface begins with the electrochemical deposition of PANI using potentiostatic deposition at 1.0 V to create a green PANI film on the electrode surface. This bare PANI surface was modified through submerging in liquid ammonia to deprotonate the polymer chain and create a blue PANI/Ammonia complex. On applying 1.0 V to the PANI/Ammonia complex in 0.9 M arginine, the polymer quickly transforms to the fully oxidized state, pernigraniline. This oxidation allows for the nucleophilic addition of arginine to the quinoid structure of PANI as described in Supporting Information SI-2 and Figure S5b. This stage of the sensing layer is the final step of fabrication and is characterized by the addition of arginine to the polymer chain and purple color visually seen, aptly described as a PANI/Ammonia/Arginine complex. The final characterization of the sensing interface is the absorption of fentanyl onto the surface and is noted as a PANI/Ammonia/Arginine/Fentanyl complex. The complete sensor was also characterized using scanning electron microscopy (SEM) and atomic force microscopy (AFM) to visualize the morphology of the interface (Figure S6). The surface was largely uniform, showing a highly porous and overlapping arrangement of fibers. The sensor interface showed no significant morphology changes and remained indistinguishable after the absorption of fentanyl onto the interface.

The computationally designed noncovalent bond pattern was further characterized by Fourier transform infrared (FTIR) spectroscopy measurements by tracking the related adsorption peaks (Figure 2a). The FTIR region between 1100 and 1700 cm^{-1} of fentanyl, arginine, and their solution composite (Fent + AS) in a 1:1 molar ratio is shown in Figure 2a. The fentanyl FTIR spectrum showed peaks at 1596 cm^{-1} for C═C aromatic stretching. Tertiary amine C−N stretching can be seen at 1136 and 1192 cm^{-1}. C−N stretching from the O═C−N group of fentanyl was observed at 1240 and 1276 cm^{-1}, respectively, confirming the N-substituted amide. These peaks confirm the fentanyl structure. Hydrogen bonds increase bond length, and their formation will result in the red shifting of absorption peaks.[38] The red shifting of the N−H in-plane bending and C−N stretching is seen in the FTIR, both of which can reasonably be attributed to hydrogen bonding between the piperidine group of fentanyl and guanidino groups of arginine. This is further supported through observation of red shifting in the formation of uracil dimers.[39] It was demonstrated that NH stretching and bending vibrations of uracil dimers resulted in variation of peaks by 49 and 22 cm^{-1}, respectively. This result corroborates our values found in the red shifting of peaks at 1276 and 1240 cm^{-1}. The aromatic

https://doi.org/10.1021/acs.analchem.2c00017
Anal. Chem. 2022, 94, 9242−9251

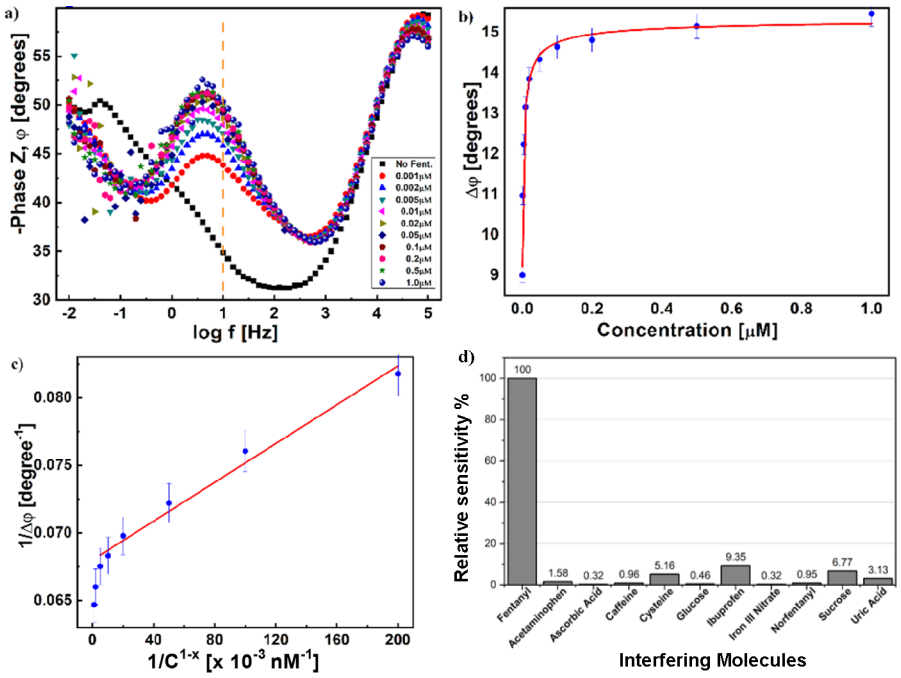

Figure 3. Sensor response and calibration in the PBS. (a) Bode plot with various concentrations of fentanyl in PBS solution. (b) Fentanyl response from Figure 2a at 10 Hz following Langmuir isotherm. (c) Linear Langmuir relationship of the sensor response in PBS. (d) Comparison of sensor sensitivity toward interfering molecules.

C═C stretching at 1590 cm^{-1} red shifted due to H−N+···π interaction between the benzene ring of fentanyl and guanidino of arginine. It has been described that cation−π interactions are overall favorable energy states.[40] This is in conjunction with the fact that protonated amines are much more likely to form favorable cation−π than neutral amines, which is important as the natural arginine zwitterion contains a protonated amine. Additionally, C−N stretching from the COO^- in arginine blue shifted at 1401 cm^{-1} indicating the strengthening of bonds upon interacting with the aromatic group of fentanyl due to cation−π interactions.

UV−vis spectroscopy in Figure 2b was utilized to confirm the sensitivity of PANI and theoretical calculations between fentanyl and the anchor site on the sensor interface. Since PANI is a conductive polymer, UV−vis spectroscopy is capable of characterizing the changes of PANI at each stage of sensor fabrication when deposited on ITO glass, supplemented by color images in Figure 2c. When observing the bare PANI sensor prior to functionalization, it is characterized as emeraldine salt PANI (green color) due to the absorbance peaks at 425 and 800 nm. These peaks represent the polaron bands and free-electron absorbance tail, respectively.[41] Submerging the bare PANI sensor with aqueous ammonia deprotonated the conductive polymer and transitions to emeraldine base (navy blue), characterized by the peaks at 350 and 640 nm and corresponds to the $\pi-\pi^*$ transition of benzenoid rings and exciton transition of quinoid rings, respectively.[41] Electrochemical deposition of arginine blue shifts the peak to 625 nm, indicating a decrease in the conjugation of the structure.[42] The absorption of fentanyl onto the sensor increases the conjugation and subsequently red shifts the absorbance peak to 655 nm. It has been demonstrated that postpolymerization substitution of PANI can be achieved by nucleophilic addition of amines while retaining its intrinsic EC properties.[43,44] However, the addition of substituents onto the conjugated backbone of PANI can introduce steric strain, thereby inducing torsion to the otherwise planar configuration of PANI, and the polymer will deviate from the optimal $\pi-\pi$ orbital overlap.[42,45] This will reduce the effective conjugation of the polymer, resulting in a decreased wavelength as seen in the UV−vis spectroscopy after the attachment of arginine as a substituent of PANI. It is consistent with the literature, which shows that the color shift in PANI toward purple is indicative of the nonconductive pernigraniline.[46] In the UV−vis spectrum, the $\pi-\pi$ stacking interaction is demonstrated upon the absorption of fentanyl on the anchor site because the wavelength was red shifted from 625 to 655 nm. It indicates that absorption of fentanyl lowers the energy state of the overall structure. This result is consistent with $\pi-\pi$ stacking observed in other complex systems.[47]

A series of quantitative UV spectroscopy measurements were also performed to confirm that the optimized molar ratio of it is 1:1 (Figure S7), which was consistent with the computational design. The interaction of arginine toward fentanyl was studied using 0.1 mM fentanyl with varying arginine concentrations (0.02−0.1 mM) in PBS solution. It was observed that at a 1:1 molar ratio of arginine to fentanyl, the absorbance shifts were at a maximum. These findings from UV−vis spectroscopy support the theoretical bonds between fentanyl and the sensor interface, securing the selectivity of the sensor developed.

iMSR Sensing Technique Analysis. Electrochemical impedance spectroscopy (EIS) is an effective technique to monitor interfacial properties.[48] In comparison to other EC techniques such as cyclic voltammetry and potentiometry, it is a nondestructive method for target molecules. EIS measures the current response when a sinusoidal potential is applied to the electrode within a frequency range. PBS was first used to establish the effectiveness of our sensor and study the

https://doi.org/10.1021/acs.analchem.2c00017
Anal. Chem. 2022, 94, 9242−9251

adsorption behavior. It was tested across multiple magnitudes of fentanyl concentration to verify the sensor design. Additionally, the wide concentration range tested also verifies the appropriateness of the sensor design outside of clinical concentrations, such as in forensic applications. Figure 3a shows the EIS response of the fabricated sensor in the PBS. The response signal is dependent on fentanyl concentration, indicating the fentanyl uptake toward the interface, and the sensor is completely covered with it.[49,50] As shown in the bode plot of EIS in PBS (Figure 3a), the phase angle changes even when a trace amount of fentanyl was added to the PBS solution, especially in the 0−10 Hz range. This is due to the strong affinity of AS toward fentanyl that increases the delocalization of charge at the interface with the specific adsorption. The charge delocalization results from two benzene rings in the fentanyl structure. However, interaction with AS further enhances this delocalization with additional positive charge resonating within the amine−amide groups in AS. This changes the electronic properties of PANI and further changes the phase angle of the system. Thus, the phase angle signal can be measured as a difference between responses (ΔR) at no fentanyl and at each fentanyl concentration. ΔR becomes significant and can be easily recorded.

The phase angle shift can be measured as a phase difference between potential and current responses. For a resistor, the phase difference is zero, and for a capacitor, the phase difference is 90°. The phase angle between 0° and 90° indicates the change in interfacial properties due to the change in resistive and capacitive properties of the system. The real capacitance defines the capacitance of the system.[51] As shown in Figure S8, the capacitance change indicates the change at the interface rather than bulk. However, in this study, PANI was used as a substrate for the sensor that shows the charge shift in the capacitive property when fentanyl adsorption occurs at the interface as designed. The interaction of AS and fentanyl results increase in charge delocalization due to their resonating structures that change the electronic structures of PANI. This compensates for the reduction in PANI signal with fentanyl detection. We noticed the phase angle (ϕ) had a better sensor response to the concentration of fentanyl than any other parameters from EIS measurements, including Z, Z′, and Z″. These little changes in capacitance due to fentanyl chemical adsorption directly influence the phase angle in the EIS measurement. According to the analysis in Supporting Information 4-1, the phase angle is proportional to the capacitance. Additionally, the phase angle is a parameter that could be directly read out through the EIS instrument without further analysis. Thus, the phase angle shift was chosen as a response for the sensor. The sensor will behave like a capacitor in the AC signal during the detection. When fentanyl coverage is increased, the charge gets delocalized at the interface upon interacting with the sensor. The interaction is behaving like a charging capacitor. The difference in potential and current signals reaches the maximum at the highest concentration and can be represented by phase angle. The increasing fentanyl results in the capacitance change. The fast-charging process indicates the current response is "catching up" with the potential response, therefore a smaller phase angle shift.

Sensor Calibration in PBS and Variable Body Fluids. As designed, the Langmuir isotherm adsorption was studied to describe the formation of a fentanyl monolayer over the surface of AS-PANI, as shown in Figure 3b. It was assumed there is a finite number of identical sites on which fentanyl monolayer forms. On the basis of this assumption, the Langmuir adsorption model can be described as[60]

$$\Delta\varphi = \frac{qK_{\mathrm{L}}C^{1-x}}{1 + K_{\mathrm{L}}C^{1-x}} \tag{1}$$

where $\Delta\varphi$ is the difference in phase angle between sensor and fentanyl interaction, q the max monolayer coverage capacity (ng deg^{-1}), K_{L} the Langmuir isotherm constant (nM^{-1}), C the concentration of fentanyl (nM), and x varies from 0 to 1. These factors can be determined by transforming the above equation into its linear form

$$\frac{1}{\Delta\varphi} = \frac{1}{q} + \frac{1}{qK_{\mathrm{L}}C^{1-x}} \tag{2}$$

The max monolayer capacity was determined from the slope and the intercept of $1/\Delta\varphi$ vs $1/q$ plot. From Figure 3c, these values were calculated as q = 306.12 ng deg^{-1} and K_{L} = 112.6 nM^{-1}. The K_{L} is the associated equilibrium constant. The $K_{\mathrm{L}} > 1$ is the indication that adsorption energy is higher than desorption which also corroborates the strong interaction between AS and fentanyl.[61] The excellent fitting to experimental results with the Langmuir model (R^2 = 0.9917) further corroborates the adsorption mechanism of fentanyl. The shape of the curve indicates the adsorption behavior is favorable under optimized conditions.[62]

The nature of adsorption also can be determined by expressing Langmuir isotherm as dimensionless constant separation factor or equilibrium parameter, R_{L}

$$R_{\mathrm{L}} = \frac{1}{1 + K_{\mathrm{L}}C_0^{1-x}} \tag{3}$$

If $R_{\mathrm{L}} > 1$, the adsorption is unfavorable. If $R_{\mathrm{L}} = 1$, the adsorption is linear. If $0 < R_{\mathrm{L}} < 1$, the adsorption is favorable, and if $R_{\mathrm{L}} = 0$, the adsorption is irreversible. The values of R_{L} in all solutions are less than 1, indicating the fentanyl adsorption on our sensor is favorable within the concentration 1−1000 nM (Figure S9), which covered not only medical needs but also other fentanyl detection such as forensic applications.

Demonstrating excellent selectivity toward fentanyl is crucial when developing a sensor utilized in POCT due to the lack of preparation prior to electrochemical analysis. The sensor interface must have a negligible response to interfering molecules to ensure that it would be robust in biological samples. To best mimic biological samples in which the sensor would be utilized, a pH = 7.4 PBS solution was selected as the electrolyte for testing, and interfering molecules were added at biologically relevant concentrations. To test the selectivity, the sensor was submerged in the PBS solution, and various concentrations of the selected analyte were added, followed by the phase angle measurement. The interfering molecules tested were glucose, sucrose, caffeine, cysteine, acetaminophen, norfentanyl, ascorbic acid, uric acid, ibuprofen, and iron(III) nitrate (Figure S10), which were chosen at human blood concentration range.[33,52−59] The relative sensitivity toward each interfering molecule is summarized in Figure 3d and was calculated by determining the absolute change in phase angle as a proportion of the baseline prior to absorption. The EIS results indicated that little interference was observed in the presence of biologically relevant molecules. The largest inference came from ibuprofen and was lower than 10%, since the selective iMSR design secures the molecule structural

https://doi.org/10.1021/acs.analchem.2c00017
Anal. Chem. 2022, 94, 9242−9251

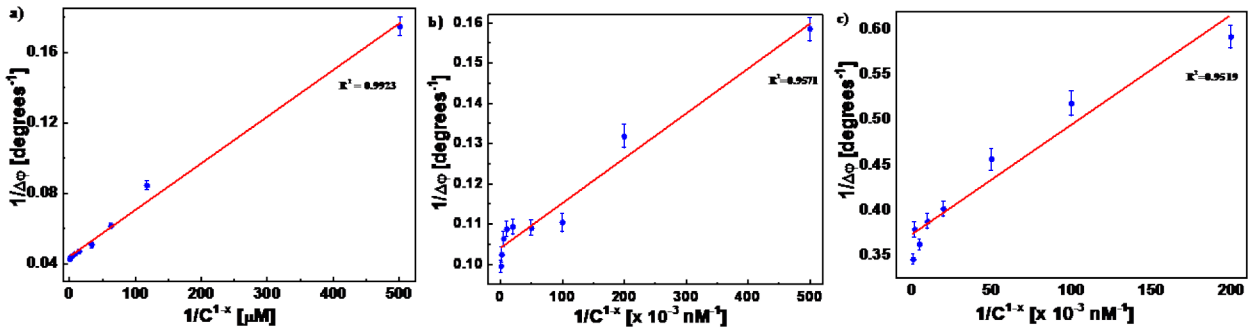

Figure 4. Linearized Languir isotherm plots for the change in phase angle at 10 Hz in (a) human serum, (b), artificial tears, and (c) artificial sweat after exposure to various concentrations of fentanyl.

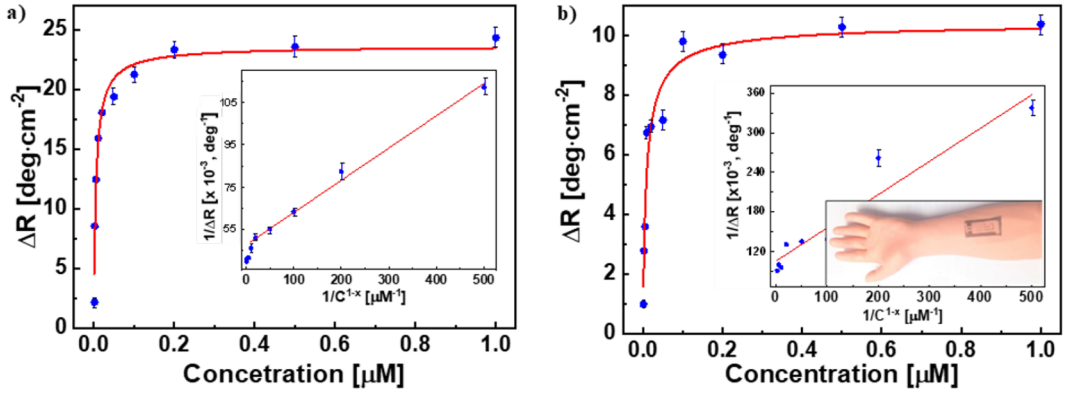

Figure 5. Flexible and attachable sensor engineered for POC clinical test. Sensor response with fixed frequency mode (10 Hz) (a) testing strip forhuman serum and (b) attachable patch for artificial sweat on artificial arm. Inset: Linear Langmuir behavior of the sensor and image showing transparency on artificial arm (b).

adsorption, and phase angle selection enhanced the sensitivity of fentanyl. These results show that the sensor interface demonstrates excellent selectivity, and minimal interference is observed when biologically relevant concentrations of interfering molecules are present.

With the calibration method established in the PBS, the sensor was further used to be applied in three common body fluids. In order to explore the possible noninvasive options of fentanyl detection, artificial tears and artificial sweat samples were selected.[63,64] A series of specific calibration curves were obtained in human serum (Figure 4a), artificial tears (Figure 4b), and artificial sweat (Figure 4c) from EIS bode plots (Figure S11) and Langmuir fitting (Table S4). There are varying amounts of precision between the three testing solutions. A serum testing solution provides the best linear relationship, followed by artificial tears and artificial sweat. The sensitivity is higher in human serum than those of artificial tears and sweat because fentanyl has a strong binding affinity to proteins present in serum. The strong binding affinity to protein is the reason that other components in serum have no interference with the detection of fentanyl. Besides, some of the electrochemically active proteins may result in increased response. The signals changed when the sensor was tested in artificial tears and sweat. The sensitivity was reduced when the sensor was used for detection in artificial tears, and artificial sweat fentanyl levels in these fluids are much lower than in human serum. This hierarchy of effectiveness is likely due to the natural buffer system present in blood that is not present in artificial tears or sweat. The bulk response of artificial tears and sweat with the low electric activity (conductivity) may contribute to the capacitance signal of PANI. Moreover, the weak buffer capability of artificial tears and the ionic nature of sweat showed more noise at higher concentrations. The buffer system acts to stabilize the pH from interfering species and maintain a constant environment. A more detailed analysis on the tear and sweat samples will be conducted in the future with human samples.

By taking advantage of the flexibility of PANI and the durability of EIS measurement, an engineered sensor with attachable subtracts for variable detection settings was fabricated. The designed sensor was used comfortably as a flexible sensor strip and on an artificial arm with fixed frequency mode (10 Hz). The time-course measurements were taken after the addition of fentanyl into the testing solution, as present in the Supporting Information (Figure S12). The response was plotted as a function of time. Addition of fentanyl into the testing solution demonstrates that the sensor interface quickly saturates and reaches 90% of the signal at a stable range within 500 s. The instrument measurements for each were taken in 2−3 s. Thus, for each fentanyl concentration, the incubation time is 500 s for the testing. The instrument responding time is about 2−3 s, and the response is shown in Figure 5 (enlarged plots). We imitated the data collection on a testing strip in which the electrode was fabricated on the polytetrafluoroethylene (PTFE) based on human serum (Figure 5a), while the transparent polydimethylsiloxane (PDMS) was used as the substrate to ensure its usage as a flexible sweat patch in monitoring the fentanyl levels on an artificial arm (Figure 5b). The response of fentanyl detection in human serum showed excellent sensitivity compared to

https://doi.org/10.1021/acs.analchem.2c00017
Anal. Chem. 2022, 94, 9242−9251

those shown in Figure 4 and has shown neglectable interference in the signal despite the complex composition of human serum, as further detailed in Figure S11. The designed sensor also showed a response when used on an artificial arm in artificial sweat. The signal response showed similar behavior to those when the sensor was tested in the artificial sweat solutions. This method will be further evaluated through the clinical samples, and the results will be presented in future publications.

The above results indicated that this assay has the potential to use as a universal platform for developing the user-driven device applicable to the variable settings. Among the current published methods (Table S5), EC-based detection has been reported several times. Compared to other EC approaches voltammetric, potentiometric, and amperometric, this method has shown higher specificity, wide detection range, and sensitivity. Due to its new molecule recognizing mechanism and AS-PANI interface design, the sensor is inherently against the interferences, thus suitable for clinical POC testing. Liquid chromatography−mass spectroscopy has been considered as the *gold standard* method for detection.[65−67] However, it needs a professional operator and significant clinical processing time (1−2 days). In addition, the detection range and limit of detection (LOD) of this sensor fully covered the clinical requirement for fentanyl detection and are extendable to high content samples. By taking advantage of the EC device, this sensor has met the clinical POCT criteria.

iMSR Sensor Clinical Validation. Twenty-three human blood samples were tested using the test strip as presented above to verify the accuracy of this assay, where LC-MS results were used as the standard method. The clinical blood sample testing was performed by adding serum sample into PBS in a 1:6 ratio. A series of experiments were performed to evaluate the possible variations from serum vs PBS and serums from different individuals. The results are shown in Figure S13. The result demonstrated the feasibility of testing the serum sample using this method. The different serum samples did not cause a significant impact on the PANI. As a result, testing in a complex environment of the human sample does not pose significant challenges when considering the nonspecific absorption of molecules. The patient human sample tests were performed in the commercial serum-stabilized PBS solution. The instrument testing time of the biosensor for each sample was 2−3 s. The scattered plot of 23 samples (including one 0 nM) is shown in Figure 6, in which each point is the mean of the triplicate measurements. The bias of the sensor against LC-MS is convergent with fentanyl concentration. At 60 nM of anesthesia cutoff concentration, the deviation is about ±5%. There was only one data point in each catalog crossing the cutoff level of about 3%, respectively, which is in the error range of general medical testing. Of the 23 samples, it caused the ratio of true positives and true negatives of the assay to be 90.9% and 91.7%. Here, true negative describes a situation where the concentration of fentanyl was correctly identified as below 60 nM, while true positive describes a situation where the concentration of fentanyl was correctly identified as above 60 nM.[68,69] Patient samples used in this work were identified and represented an inclusive population of individuals which had varying concentrations of sugars and fats in their serums. The small variation in % bias indicates that the diverse set of samples tested does not interfere with the sensor response. It is noted that such values of sensitivity and specificity of detection method for small

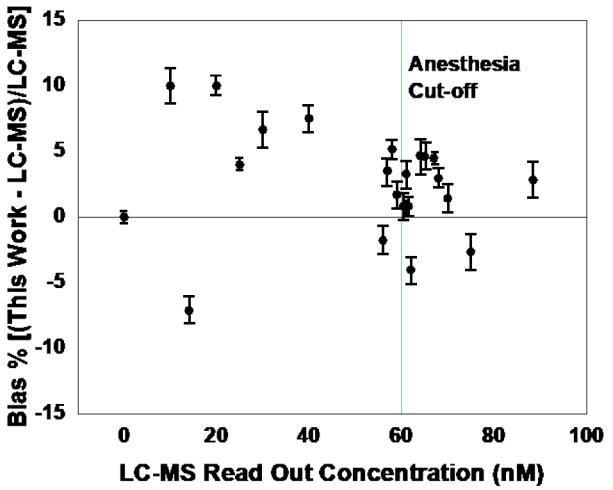

Figure 6. Statistical clinical human blood strip test compared to LC-MS. The scatter plot displays how detection results are distributed in negative and positive groups, and each point is the mean of the triplicate measurements.

molecules with an EC flexible POCT setting have not been reported to date. The assay with the oral fluids and skin patch clinical monitoring is under processing, and the results will be presented in future publications.

CONCLUSIONS

In this work, we have demonstrated a new POCT fentanyl assay, in which a sensing anchor layer was designed to enable multiple noncovalent bonds with fentanyl molecules and achieved 1:1 structural adsorption. Incorporating with a conducting polymer PANI transductor, the phase angle in the differential EIS, which was used as the sensor technique, has inherently amplified signals compared to changes in resistance, potential, and/or current signals during this specific adsorption. The extra selectivity was produced by this high EIS response, then would be caused by other possible species at the same condition. By taking advantage of the flexibility of PANI and the durability of the EIS measurement, the new interface of biocompatible and flexible composite layers can be fabricated via the EC approach on a variety of surfaces. This approach is particularly useful for assays that require extremely low sample volumes for testing strips/vials for tear and blood samples and testing patches through skin perspiration. In all three body fluids, this iMSR sensor showed excellent sensitivities and wide linear behavior in the fentanyl range from 0.1 to 1000 nM in serum, 0.5 to 500 nM in artificial tears, and 1 to 200 nM in artificial sweat, which would meet the needs for both pharmaceutical measurement and clinical testing. The iMSR sensor showed excellent sensitivity in the clinical concerned concentration range with very low interferences. In 23 blood tests from clinical patients, the deviation of test results is about ±5% in comparison with method LC-MS at 60 of an anesthesia cutoff concentration. However, the responding time of the iMSR sensor only took a few seconds.

Since this high selectivity and sensitivity method was fundamentally designed and crafted with molecular-level functional group recognition, it overcomes the major barrier of biosensors for practical applications. The EIS test employed in this work has a low requirement on the power sources and frequency settings, and all parameters could be read out

https://doi.org/10.1021/acs.analchem.2c00017
Anal. Chem. 2022, 94, 9242−9251

directly without further analysis. In order to make our sensor design compatible with a point-of-care setting, careful consideration must be taken in order to verify the accessibility of platforms in which our sensor is compatible, including the electrode, control device, and more. When looking at the required instrumentation, the platform could be portable, cost effective, and enable real-time results with this method. Phones and mobile devices in recent years pose an excellent opportunity to fulfill these requirements and push forward many POC sensors into operation. In addition, success has already been seen with the realization of impedance-based sensors powered through mobile devices. As a result, proper development of a sensing platform through mobile devices and related method optimization will allow widespread implementation of POC sensors as described in this work and others. This small molecule recognition proof of concept, based on iMSR, may provide such a robust and highly selective approach for POC small molecule drug and biomarker detection as a promising separation-free sensory methodology.

■ ASSOCIATED CONTENT

Supporting Information

The Supporting Information is available free of charge at https://pubs.acs.org/doi/10.1021/acs.analchem.2c00017.

SI-1: Computational methodology with four zwitterionic isomers of arginine, optimized geometries. Calculated binding energy values for all adsorption complex configurations. Summary statistics for calculated binding energy values. One-way analysis of variance (ANOVA) of calculated binding energy values. Calculated binding energy values for all adsorption complex configurations and box and whisker plots for calculated binding energy values for all adsorption complex configurations. SI-2: PANI structure and functionalization exerpiemental method. SI-3: Sensor characterizations including SEM, AFM images, and UV spectra. SI-4: Sensor tests including capacitance vs frequency response and EIS analysis, adsorption curves, all sensor selectivity data, calibration/Langmuir data at variable body fluids, saturation of signal for fentanyl addition, current method comparison table, and time-course stabilization curve. (PDF)

■ AUTHOR INFORMATION

Corresponding Author

Zhe Wang − *Chemistry Department, Oakland University, Rochester, Michigan 48309, United States;* orcid.org/0000-0003-3762-3167; Email: zhewang@oakland.edu

Authors

Amit Nautiyal − *Department of Chemistry, Xavier University of Louisiana, New Orleans, Louisiana 70125, United States*

Christopher Alexopoulos − *Chemistry Department, Oakland University, Rochester, Michigan 48309, United States*

Rania Aqrawi − *Chemistry Department, Oakland University, Rochester, Michigan 48309, United States*

Xiaozhou Huang − *Department of Mechanical Engineering, George Mason University, Fairfax, Virginia 22030, United States*

Ashraf Ali − *Department of Chemical Engineering, Auburn University, Auburn, Alabama 36849, United States*

Katherine E. Lawson − *Department of Chemical Engineering, Auburn University, Auburn, Alabama 36849, United States*

Kevin Riley − *Department of Chemistry, Xavier University of Louisiana, New Orleans, Louisiana 70125, United States*

Andrew J. Adamczyk − *Department of Chemical Engineering, Auburn University, Auburn, Alabama 36849, United States*

Pei Dong − *Department of Mechanical Engineering, George Mason University, Fairfax, Virginia 22030, United States*

Xinyu Zhang − *Department of Chemical Engineering, Auburn University, Auburn, Alabama 36849, United States;* orcid.org/0000-0003-3830-4096

Complete contact information is available at: https://pubs.acs.org/10.1021/acs.analchem.2c00017

Author Contributions

Z.W. and X.Z. conceived the study. Z.W., A.N., C.A., and R.A. acquired experimental data. P.D. and X.H. developed the attachable device. A.J.A, A.A., and K.E.L. acquired the computational data. Z.W. and A.N. wrote the first draft of the manuscript with substantial contributions from P.D., X.H., A.J.A., K.R., and X.Z. All authors edited and approved the final version of the manuscript.

Notes

The authors declare no competing financial interest.

■ ACKNOWLEDGMENTS

This publication was made possible by the support from the Army Research Office (W911NF-18-1-0458), National Science Foundation (CHE-1832167, HRD-1700429, and HRD-1505219). Z.W. acknowledges the startup funding, URC Faculty Research Fellowship, and REF Research grant from Oakland University and Michigan Space Grant Consortium. P.D. acknowledges the financial support of the startup funding from George Mason University, United States. The authors would like to thank Surah Srinivas, Brooke Nguyen, and Brianna Burton for their data collection contributions and especially Dr. Maria Bryant for her helpful suggestions.

■ REFERENCES

(1) Dasgupta, N.; Beletsky, L.; Ciccarone, D. *American journal of public health* **2018**, *108* (2), 182−186.

(2) Cicero, T. J.; Ellis, M. S. *Dialogues in clinical neuroscience* **2017**, *19* (3), 259.

(3) Rose, M. E. *Pain Med.* **2018**, *19*, 793.

(4) Wickramatilake, S.; Zur, J.; Mulvaney-Day, N.; Klimo, M. C. v.; Selmi, E.; Harwood, H. *Public Health Reports* **2017**, *132* (2), 171−179.

(5) Sullivan, M. D.; Turner, J. A.; DiLodovico, C.; D'Appollonio, A.; Stephens, K.; Chan, Y. F. *J. Pain* **2017**, *18* (3), 308−318.

(6) Dowell, D.; Haegerich, T. M. *Ann. Int. Med.* **2017**, *167* (3), 208−209.

(7) Katz, J.; Goodnough, A. The Opioid Crisis Is Getting Worse, Particularly for Black Americans. *New York Times*; December 22, 2017.

(8) Volkow, N. D.; Collins, F. S. *New Engl J. Med.* **2017**, *377* (4), 391−394.

(9) Rummans, T. A.; Burton, M. C.; Dawson, N. L. *Mayo Clinic Proceedings* **2018**, *93*, 344−350.

(10) Madras, B. K. *Clin Pharmacol Ther* **2018**, *103* (6), 943−945.

(11) Spencer, M.; Warner, M.; Bastian, B.; Trinidad, J.; Hedegaard, H. *Nal. Vital Stat. Rep.* **2019**, *68*, 1−19.

(12) *Carfentanil: A Dangerous New Factor in the U.S. Opioid Crisis*; National Center on Safe Supportive Learning Environments, 2016.

(13) Gill, J. R.; Lin, P. T.; Nelson, L. *Journal of medical toxicology* **2013**, *9* (1), 34−41.
(14) Alkharfy, K. M.; Frye, R. F. *J. Chromatogr B Biomed Sci. Appl.* **2001**, *753* (2), 303−8.
(15) Li, W.; Tse, F. L. S. *Biomedical Chromatography* **2010**, *24* (1), 49−65.
(16) Thomasy, S. M.; Mama, K. R.; Stanley, S. D. *Journal of Analytical Toxicology* **2008**, *32* (9), 754−759.
(17) Mirsafavi, R.; Moskovits, M.; Meinhart, C. *Analyst* **2020**, *145* (9), 3440−3446.
(18) Shende, C.; Farquharson, A.; Brouillette, C.; Smith, W.; Farquharson, S. *Molecules* **2019**, *24* (14), 2578.
(19) Haddad, A.; Comanescu, M. A.; Green, O.; Kubic, T. A.; Lombardi, J. R. *Anal. Chem.* **2018**, *90* (21), 12678−12685.
(20) Alharbi, O.; Xu, Y.; Goodacre, R. *Analyst* **2015**, *140* (17), 5965−5970.
(21) Wilson, A. D.; Baietto, M. *Sensors* **2009**, *9* (7), 5099−5148.
(22) de Jong, M.; Sleegers, N.; Kim, J.; Van Durme, F.; Samyn, N.; Wang, J.; De Wael, K. *Chemical Science* **2016**, *7* (3), 2364−2370.
(23) Wang, J. *TrAC Trends in Analytical Chemistry* **2002**, *21* (4), 226−232.
(24) Thevenot, D. R.; Tóth, K.; Durst, R. A.; Wilson, G. S. *Pure Appl. Chem.* **1999**, *71* (12), 2333−2348.
(25) Ferreira, P. C.; Ataíde, V. N.; Silva Chagas, C. L.; Angnes, L.; Tomazelli Coltro, W. K.; Longo Cesar Paixão, T. R.; Reis de Araujo, W. *TrAC Trends in Analytical Chemistry* **2019**, *119*, 115622.
(26) Takahashi, S.; Sugimoto, N. *Acc. Chem. Res.* **2021**, *54* (9), 2110−2120.
(27) Miyoshi, D.; Nakamura, K.; Tateishi-Karimata, H.; Ohmichi, T.; Sugimoto, N. *J. Am. Chem. Soc.* **2009**, *131* (10), 3522−3531.
(28) Grimme, S. *J. Chem. Phys.* **2006**, *124* (3), 034108.
(29) Langreth, D. C.; Mehl, M. J. *Phys. Rev. B* **1983**, *28* (4), 1809−1834.
(30) Grimme, S.; Antony, J.; Ehrlich, S.; Krieg, H. *J. Chem. Phys.* **2010**, *132* (15), 154104.
(31) Andzelm, J.; Kölmel, C.; Klamt, A. *J. Chem. Phys.* **1995**, *103* (21), 9312−9320.
(32) Liu, Q.; Liu, Y.; Wu, F.; Cao, X.; Li, Z.; Alharbi, M.; Abbas, A. N.; Amer, M. R.; Zhou, C. *ACS Nano* **2018**, *12* (2), 1170−1178.
(33) Zhang, Y.; Huang, Z.; Wang, L.; Wang, C.; Zhang, C.; Wiese, T.; Wang, G.; Riley, K.; Wang, Z. *Anal. Chem.* **2018**, *90* (7), 4733−4740.
(34) Gallivan, J. P.; Dougherty, D. A. *J. Am. Chem. Soc.* **2000**, *122* (5), 870−874.
(35) Janiak, C. *J. Chem. Soc., Dalton Trans.* **2000**, *21*, 3885−3896.
(36) Halder, A.; Data, D.; Seelam, P. P.; Bhattacharyya, D.; Mitra, A. *ACS Omega* **2019**, *4* (4), 7354−7368.
(37) Nautiyal, A.; Cook, J. E.; Zhang, X. *Prog. Org. Coat.* **2019**, *136*, 105309.
(38) Kubelkova, L.; Kotrla, J.; Florian, J. *J. Phys. Chem.* **1995**, *99* (25), 10285−10293.
(39) Fornaro, T.; Burini, D.; Biczysko, M.; Barone, V. *J. Phys. Chem. A* **2015**, *119* (18), 4224−4236.
(40) Gallivan, J. P.; Dougherty, D. A. *Proc. Natl. Acad. Sci. U. S. A.* **1999**, *96* (17), 9459−9464.
(41) Kuo, C.-W.; Kuo, Z.-Y.; Jow, J.-J.; Wu, T.-Y.; Chen, J.-Y.; Zhu, X.-X. *Int. J. Electrochem. Sci.* **2012**, *7*, na.
(42) Martínez-Sánchez, B.; Cazorla-Amorós, D.; Morallón, E. *Polymers* **2020**, *12* (12), 2820.
(43) Yang, D.; Zuccarello, G.; Mattes, B. R. *Macromolecules* **2002**, *35* (20), 7856−7856.
(44) Cook, J. *Surface Engineering of Organic Conductors*. Ph.D. Thesis, Auburn University, 2018.
(45) Andriianova, A. N.; Biglova, Y. N.; Mustafin, A. G. *RSC Adv.* **2020**, *10* (13), 7468−7491.
(46) Jamadade, V. S.; Dhawale, D. S.; Lokhande, C. D. *Synth. Met.* **2010**, *160* (9), 955−960.
(47) Ostrowska, K.; Ceresoli, D.; Stadnicka, K.; Gryl, M.; Cazzaniga, M.; Soave, R.; Musielak, B.; Witek, L. J.; Goszczycki, P.; Grolik, J.; Turek, A. M. *IUCrJ.* **2018**, *5* (3), 335−347.
(48) Balasubramani, V.; Chandraleka, S.; Rao, T. S.; Sasikumar, R.; Kuppusamy, M. R.; Sridhar, T. M. *J. Electrochem. Soc.* **2020**, *167* (3), 037572.
(49) Rout, T. K.; Jha, G.; Singh, A. K.; Bandyopadhyay, N.; Mohanty, O. N. *Surf. Coat. Technol.* **2003**, *167* (1), 16−24.
(50) Bautista, A.; González, J. A.; Otero, E.; Morcillo, M.; Almeida, E. *Discrimination by EIS of Degradation Mechanisms in Lap Joints of Coated Metal Sheet*; Springer, 1999.
(51) Orazem, M. E.; Tribollet, B. *Electrochemical Impedance Spectroscopy*, 2nd ed.; Wiley, 2017.
(52) The Emerging Risk Factors Collaboration. *Lancet* **2010**, *375* (9733), 2215−2222.
(53) Willson, C. *Toxicol Rep* **2018**, *5*, 1140−1152.
(54) Rehman, T.; Shabbir, M. A.; Inam-Ur-Raheem, M.; Manzoor, M. F.; Ahmad, N.; Liu, Z.-W.; Ahmad, M. H.; Siddeeg, A.; Abid, M.; Aadil, R. M. *Food Science & Nutrition* **2020**, *8* (9), 4696−4707.
(55) Poklis, J.; Poklis, A.; Wolf, C.; Mainland, M.; Hair, L.; Devers, K.; Chrostowski, L.; Arbefeville, E.; Merves, M.; Pearson, J. *Forensic science international* **2015**, *257*, 435−441.
(56) Hagel, A. F.; Albrecht, H.; Dauth, W.; Hagel, W.; Vitali, F.; Ganzleben, I.; Schultis, H. W.; Konturek, P. C.; Stein, J.; Neurath, M. F.; Raithel, M. *J. Int. Med. Res.* **2018**, *46* (1), 168−174.
(57) Desideri, G.; Castaldo, G.; Lombardi, A.; Mussap, M.; Testa, A.; Pontremoli, R.; Punzi, L.; Borghi, C. *Eur. Rev. Med. Pharmacol Sci.* **2014**, *18* (9), 1295−1306.
(58) Janssen, G. M. E.; Venema, J. F. *Journal of International Medical Research* **1985**, *13* (1), 68−73.
(59) Soldin, O. P.; Bierbower, L. H.; Choi, J. J.; Choi, J. J.; Thompson-Hoffman, S.; Soldin, S. J. *Clin. Chim. Acta* **2004**, *342* (1−2), 211−217.
(60) Hanaor, D. A. H.; Ghadiri, M.; Chrzanowski, W.; Gan, Y. *Langmuir* **2014**, *30* (50), 15143−15152.
(61) Ruthven, D. M. *Principles of Absorption and Adsorption Processes*; Wiley, 1984.
(62) Weber, T. W.; Chakravorti, R. K. *AIChE J.* **1974**, *20* (2), 228−238.
(63) Schneider, S.; Ait-m-bark, Z.; Schummer, C.; Lemmer, P.; Yegles, M.; Appenzeller, B.; Wennig, R. *Journal of Analytical Toxicology* **2008**, *32* (3), 260−264.
(64) Clifford, A.; Das, J.; Yousefi, H.; Mahmud, A.; Chen, J. B.; Kelley, S. O. *J. Am. Chem. Soc.* **2021**, *143* (14), 5281−5294.
(65) Sohouli, E.; Keihan, A. H.; Shahdost-fard, F.; Naghian, E.; Plonska-Brzezinska, M. E.; Rahimi-Nasrabadi, M.; Ahmadi, F. *Materials Science and Engineering: C* **2020**, *110*, 110684.
(66) Boleda, M. R.; Galceran, M. T.; Ventura, F. *Journal of Chromatography A* **2007**, *1175* (1), 38−48.
(67) Palmquist, K. B.; Swortwood, M. J. *Forensic Science International* **2019**, *297*, 189−197.
(68) Leber, W.; Lammel, O.; Siebenhofer, A.; Redlberger-Fritz, M.; Panovska-Griffiths, J.; Czypionka, T. *eClinicalMedicine* **2021**, *38*, 101011.
(69) Kim, H.; Seong, W.; Rha, E.; Lee, H.; Kim, S. K.; Kwon, K. K.; Park, K.-H.; Lee, D.-H.; Lee, S.-G. *Biosens. Bioelectron.* **2020**, *170*, 112670.

https://doi.org/10.1021/acs.analchem.2c00017
Anal. Chem. 2022, 94, 9242−9251